Engineering with Computers (2023) 39:3941–3954
https://doi.org/10.1007/s00366-023-01853-4

ORIGINAL ARTICLE

CFD-FEA based model to predict leak-points in a 90-degree pipe elbow

Ahmed A. Abuhatira[1] · **Salim M. Salim**[2] · **Jan B. Vorstius**[3]

Received: 3 October 2022 / Accepted: 17 May 2023 / Published online: 3 June 2023

Abstract

The aim of this paper is to numerically investigate Vibration-Based Leak Detection (VBLD) method in pipeline systems based on Fluid–Structure Interaction (FSI) analysis to predict leakages. In previous investigations, laboratory tests were widely used to study the VBLD technique in small-diameter water loop system pipes. The current project uses Ansys Workbench to extend these findings by integrating Computational Fluid Dynamics (CFD) with Finite Element Analysis (FEA). The study outlines a numerical method for VBLD to identify leakages in a 90-degree pipe elbow by predicting variations in vibration signals, with applications in the oil and gas industry. Firstly, changes in fluid behaviour (centrifugal force, pressure drop, secondary flow, and frictional force) experienced in the internal pipe wall resulting from a probable leakage (modelled as an additional outlet) are determined using CFD. Subsequently, the CFD results are coupled with FEA to model structural responses of the pipe walls subjected to different forces. This in turn allows the variations in vibration signals to be measured. The numerical approach presented in this paper based on FSI and incorporating the VBLD method provides a practical and convenient early detection tool that can complement physical vibration monitoring equipment in the field.

Keywords VBLD · CFD · Turbulence modelling · Pipe flow · FEA · FSI

Symbol of letters

D	Pipe diameter (m)
L	Length (m)
E	Young's modulus of the pipe (N/m^2)
$\overline{u}$	Mean value of fluid velocity (m/s)
$u_i^{'}$	Fluctuating value of fluid velocity (m/s)
$\overline{p}$	Mean value of fluid pressure (Pa)
$p_i^{'}$	Fluctuating value of fluid pressure (Pa)
ΔP	Pressure loss (Pa)
t	Time (s)
ρ	Density (kg/m^3)
v	Kinematic viscosity (m^2 s^{-1})
μ	Dynamic viscosity (Kgm^{-1} s^{-1})
R_e	Reynolds number (dimensionless quantity)
$\overline{\rho u_i^{'} u_j^{'}}$	Reynolds stresses (Pa)
τ_{ij}	Reynolds Stress tensor (Pa)
τ_w	Wall shear stress (Pa)
x_i	Distance [tensor form] (m)
f	Darcy friction factor (dimensionless quantity)
ε/D	Pipe relative roughness (mm)
F_s	Moody friction factor (dimensionless quantity)
R_b	Pipe bend radius (m)
θ	Pipe bend angle (degree)
k_b	Loss coefficient of bend pipe (dimensionless quantity)
R_c/D	Curvature radius ratio of the pipe (dimensionless quantity)
y^+	Wall dimensionless unit (dimensionless quantity)
u	Pipe surface displacement (m)
$\dot{u}$	Pipe surface velocity (m/s) = $(\frac{du}{dt})$
$\ddot{u}$	Pipe surface acceleration (m/s^2) = $(\frac{d^2u}{dt^2})$
M	Mass matrix
C	Damping matrix
K	Stiffness matrix
f	Frequency (Hz)

Abbreviations

CFD	Computational fluid dynamic
VBLD	Vibration-based leak detection

✉ Ahmed A. Abuhatira
ahmeda@lcwc.ac.uk

Salim M. Salim
s.m.salim@swansea.ac.uk

Jan B. Vorstius
j.b.vorstius@dundee.ac.uk

[1] Nuclear, HE Engineering and Science, Lakes College West Cumbria, Workington, UK

[2] Faculty of Science and Engineering, Swansea University, Swansea, UK

[3] School of Science and Engineering, University of Dundee, Dundee, UK

FSI	Fluid–structure interaction
FIV	Flow-induced vibration
RANS	Reynolds-averaged Navier–Stokes
RSM	Reynolds stress model
LES	Large eddy simulation
FEA	Finite element analysis
RMS	Root mean square
FFT	Fast Fourier transform
DOF	Degree of freedom
GIT	Grid independence test
BS	Baseline system
LS	Leak severity
LQA	Leak quantification assessment

1 Introduction

Several pipeline leak detection methods have been developed and tested over the last few decades based on various principles and approaches such as acoustic emissions [1, 2], fibre optic sensors [3, 4], pressure based methods [5–7], ground penetration radar [8, 9], dynamic modelling [6, 10], and mass volume balance [11, 12]. These methods have been classified in different ways, for instance, some researchers have divided them into two main categories namely hardware and software-based approaches [13, 14]. While other researchers have distinguished the methods based on technical aspects and categorised them into three main groups: internal, external, and non-technical methods [14, 15].

Adegboye et al.[16] recently conducted a comprehensive literature review on pipeline monitoring and leak detection techniques employed in the oil and gas sector. The work discussed different approaches and summarised the current state of the art, including the strengths and weaknesses of each technique. A comparative performance analysis was also carried out to suggest the most suitable approach for specific operating conditions. Adegboye et al. [16], then classified the different leakage detection methods into three main categories: exterior methods, visual/biological methods, and interior/computational methods. The exterior approach uses numerous man-made sensing systems attached to the outer surface of pipelines to physically detect leaks. Visual method can be carried out by a trained and experienced worker to detect leakages whereas, the interior approach employs software-based methods.

It's worth noting that although several leak detection techniques have been developed over the years, each approach has limitations and may only be appropriate for certain applications and/or be imprecise [17]. Since pipelines are generally favoured as a safer and cheaper way of transportation compared to trucks and tankers [18], there is a desire to enhance existing leak detection methods of pipeline systems.

Vibration-Based Leak Detection (VBLD) method has been introduced as one effective way of overcoming the limitations of the previously employed acoustic approach. The relative performance between the two methods was compared in an experimental study, and it was determined that vibration sensors are more accurate than acoustic sensors when it came to detecting and locating leakages in pipelines [19]. The advantageous characteristics of the VBLD technique are its sensitivity to small changes, low maintenance and cheaper running costs. The VBLD method detects early signs of leakages by using accelerometers to monitor fluctuations in vibration signal as a consequence of any changes in flow behaviour. The sensors are mounted on the pipeline external surface and connected to a computer software [19]. Other researchers have also concluded that the VBLD approach is highly reliable for early leak detection and is popular because of its non-invasive nature [16, 20, 21].

The VBLD principle relies on Fluid–Structure Interaction (FSI) phenomena [22–24], and to understand it requires a sufficient knowledge of the fluid flow behaviour and the effect on the pipe structure. Since our research is focused on the VBLD approach, we will be discussing the concept in greater detail. Additionally, we will be drawing from numerous research studies in this area.

We will start by briefly looking at the history of the gradual introduction of vibration-based approaches in monitoring and detecting leakage in pipelines. Back in 2010, Shinozuka et al. [10], proposed a new method using maximum pipe acceleration gradient (MPAG) instead of the widely used maximum water head gradient (MWHG) at that time. The study was conducted experimentally on a small diameter pipe water network and concluded that external acceleration monitoring could effectively replace the expensive process of water pressure monitoring using invasive pressure gauges.

In a 2014 study, Ismail et al. [25], proposed a monitoring technique for water pipeline systems using six degrees of freedom (DOF) accelerometer sensors (MPU6500) to detect pipes with and without leakage. The experimental investigation was conducted on a small diameter pipe water network, and they observed an inverse relationship between water pressure and pipe vibration, making it difficult to distinguish between normal and abnormal states, particularly at high pressure. But at low pressure they determined that vibration sensors were effective for detecting pipe leakage.

The same year, Martini et al. [26], experimentally evaluated the performance of vibration monitoring for leak detection and established the specifications for prototypal acquisition equipment. The study found that suitable statistics derived from raw acceleration data could be used to detect burst leaks as long as the system was free of external disturbances. The preliminary findings were used to design acquisition equipment and implement a prototypal detection algorithm.

The following year, Martini, Troncossi and Rivola [27], launched a larger experimental program to collect vibration data from actual burst leaks discovered and fixed in the water distribution network utility. The study confirmed the effectiveness of the previously proposed prototype algorithm for leak detection. As the approach was based on a basic standard deviation calculation of the raw signals, it was relatively simple to build and required very little computer power. With the use of adequate band-pass filters, all the analysed leaks were detected satisfactorily.

In 2017, Yazdekhasti et al. [28], developed an enhanced method for detecting leaks. This was achieved by continuously monitoring changes in the correlation between surface acceleration measured at discrete points along the pipeline length. The experimental study established a leak detection index (LDI) to identify the onset and subsequently analyse the severity of leaks based on the cross-spectral density of observed pipe surface accelerations. LDI was successfully shown to be sensitive to leak-induced signals while being impervious to out-of-control external disturbances. The study also found a strong link between LDI and leak severity. The following year, Yazdekhasti et al. [29], extended the investigation of the LDI-based approach on a more complex experimental set-up that included bends, T-joints, numerous loops, multiple pipe sizes, and multiple leaks. They concluded that detecting leakages in more complex pipeline networks was challenging.

Okosun et al. [30], presented another novel method in 2019. They implemented piezoelectric sensors that transformed strains from vibration into electrical signals. The approach used vibration sensing to detect, monitor, and localise water pipe breaches ranging from minor leaks to burst leaks at various flow rates. Their findings suggested that piezoelectric sensors could be used to satisfy three of the four goals of structural health. Building on this work, Okosun et al. [31], went on to develop a numerical model using CFD and FEA and compared it to existing experimental studies in a controlled laboratory setting. In 2020, they numerically validated their model and provided guidance for parameter selection and modelling. They successfully demonstrated the repeatability of results and showed that their numerical model could determine the best distribution frequency of sensors, enabling the detection of the smallest leak of consequence under a known or established flow condition.

More recently, Yang et al. [32], introduced a comprehensive leak monitoring approach in a 2022 study that enables simultaneous leak detection, localisation, and volume rate estimation in above-ground liquid pipelines. The researchers experimentally and numerically validated their method and found that the amplitude of vibration could be utilised to estimate the leak volume rate without needing to know the matching flow rate beforehand in the event of a leak. The researchers developed a leak-induced vibration model, which adequately represented the leak force and found that the size of an actual leak force and the volume flow rate of leakage were empirically related.

While acknowledging the above-mentioned studies and several trials that demonstrate the effectiveness of VBLD methods, it is worth noting that there are still gaps in the research literature, for example, in relation to computational modelling and shortage of research into large-diameter pipes. Additionally, there are questions about the applicability of the VBLD approach in the oil and gas industry, particularly in large-diameter 90-degree pipe elbows, where the flow regime is complex and difficult to quantify.

Computational modelling is presented in this study to explore the VBLD approach in 90-degree pipe elbow with applications in the oil and gas industry. This study was carried out by investigating the pipe Flow-Induced Vibration (FIV) in normal (without leak) and abnormal (different leak scenarios) conditions. Based on the conclusions and recommendations from our previously published study [34] of the wall y^+ approach, Reynolds Stress Model (RSM) is coupled with a FEA to simulate the FSI using one-way coupling. The employed RSM turbulence model and subsequent FSI approaches are initially validated against published experimental and numerical results.

The current study focuses on the flow behaviour and detection of probable leakages in a 90-degree pipe elbow, which is common in many piping systems including those widely used in the oil and gas industry. According to observations by Ejeh et al. [33], an increase in pipe curvature angle results in an increase in erosion rate. This implies that potential leakage could occur at other elbow angles ranging anywhere between 0–180 degrees, with some curvature angles being more critical than others. The same study included a sensitivity analysis which concluded that the erosion rates are influenced by particle flow rate, mass, and density. For further details refer to the comprehensive article by Ejeh et al.

2 Model description and simulation procedures

This study is designed to investigate the turbulent pipe FIV under several scenarios including a state without leaks and incidences of leaks with different severities based on their sizes. The purpose of this, is to explore the VBLD approach and find out if its capable of assessing leakages with different damage severities (small or large) in 90-degree pipe elbows, in which, the flow regime is complex and difficult to be simply characterized. Data was collected from Mellitah Oil and Gas Company, Libya for this computational study. This includes the fluid (crude oil) properties, flow

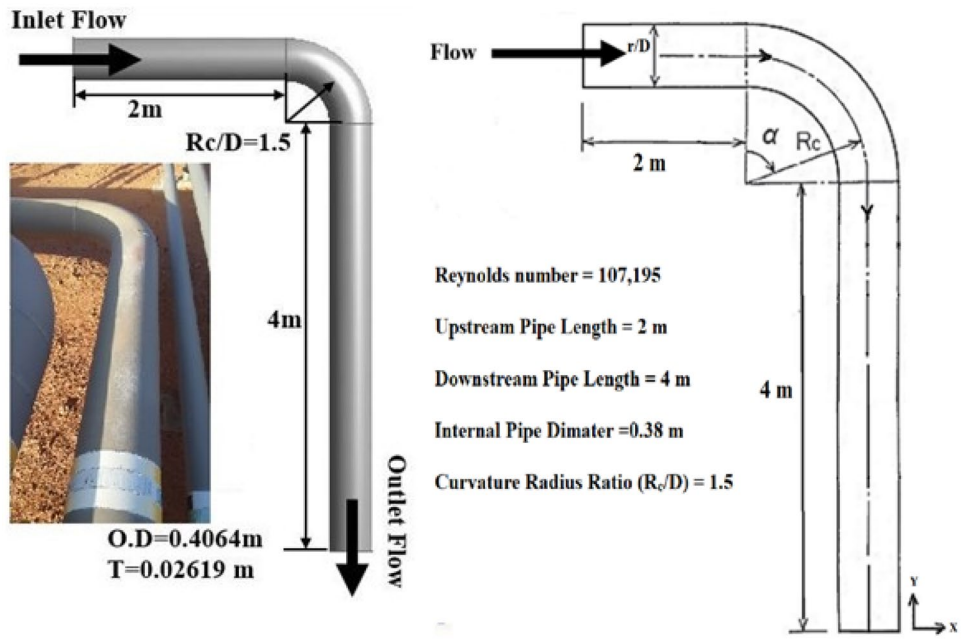

Fig. 1 Computational domain of the 90-degree pipe elbow

Table 1 Fluid properties

Fluid properties	Crude oil
Density	694 kg/m^3
Viscosity	0.00122 Pa.s
Specific gravity	0.696
Pressure	4e + 6 Pa
Velocity	0.5 m/s

Table 2 Pipeline material specifications

Pipe schedule	Material	Outer diameter (O.D)	Wall thickness
SCH100	Carbon Steel	0.4064 m	0.02619 m

rate, Reynolds number, pipeline material specifications, pipe elbow features and supports. The computational domain is illustrated in Fig. 1.

The 90-degree pipe segment is composed of an upstream pipe with a length of 2 m and a downstream pipe 4 m in length connected to a 90-degree elbow with a 1.5 curvature radius ratio (R_c/D). The velocity of the crude oil in the pipe is 0.5 m/s (constant) with a Reynolds number of 107,195. The flow is assumed to be steady, fully developed flow, and incompressible in this study. The light crude oil is a Newtonian fluid [37], with fluid properties (light crude oil) are presented in Table 1.

The pipe segment is simply supported at both ends. The pipeline system specifications including the material type, pipe diameter and pipe thickness are presented in Table 2.

One-way FSI coupling technique is used to model fluid–structure interaction. It is assumed that the fluid flow affects the structure, but the structure does not significantly impact the fluid flow. Ansys Workbench software is used to perform this one-way FSI coupling analysis. The FEA model of the structure is created in Ansys Mechanical, and the CFD model of the fluid flow is created in Ansys Fluent. The FSI analysis system is then used to transfer the results of the fluid flow simulation from the CFD model to the structural FEA model. The coupling between the fluid and structure is defined as a one-way coupling, where the fluid is treated as a load on the structure and the structure is treated as a rigid body that is not affected by the fluid flow. The simulation calculates the deformation of the structure due to the fluid load and the resulting displacement of the fluid flow, which is used to predict the pipe dynamic behaviour in a form of vibration signal. This technique was performed for all cases scenarios including a state without leaks and incidences of leaks with different severities based on their sizes. The simulations were carried out for horizontal pipe flow and gravity force was taken into consideration (activated) when employed the RANS turbulence modelling. The CFD (fluid domain) and FEA (structure domain) setups and simulations are presented in detail next.

2.1 Fluid domain

Fluid domain simulation is the first part of the FSI problem that deals with turbulent pipe flow. In a 90-degree pipe elbow, the main forces of fluid flow are caused by changes in velocity and direction of the fluid. These forces include centrifugal force, pressure drop, secondary flow, frictional force, and gravity force. Centrifugal force is due to the fluid being forced outward towards the outer edge

of the bend, while pressure drop is caused by the changes in velocity and direction. Secondary flow patterns, such as swirling or vortices, can further increase turbulence and pressure drop. Finally, the fluid experiences frictional forces due to the friction between the fluid and the inner surface of the elbow, which can lead to energy loss and decreased flow rate. Understanding these forces is important for optimizing pipe design and ensuring efficient fluid transport. Consequently, complexity arises from the internal pipe wall pressure fluctuating due to alterations in flow field parameters caused by the 90-degree elbow, and extra effort was needed to characterise it.

To balance between the accuracy of numerical solutions and computational costs, an appropriate mesh configuration should be carefully selected. Therefore, the wall y^+ approach which previously published by Abuhatira et al. [34] is implemented to balance between the computational cost and time. This technique builds on the recommendations of previous studies by Salim et al.[35–37] for using wall y^+ approach as guidance for reliable mesh and turbulence model selection in bent pipe flow studies. This approach is proposed to also reduce the time spent on the grid independence test (GIT) which involves time-consuming procedures. The wall y^+ approach has previously been shown to be successful in selecting an appropriate near wall treatment and corresponding turbulence model, and it might remove the necessity of physical validation when experimental data is unavailable or is difficult to obtain. Therefore, while also considering the recommendations from the recently published paper by the same authors [34] of the wall y^+ approach, the RSM that solves the viscous sublayer was used to investigate the turbulent pipe flow with a 90-degree elbow of crude oil. The wall y^+ value was strictly controlled to be within the viscous sublayer (≈ 5) by generating a fine mesh near the wall. This is illustrated in Fig. 2.

In addition to the important numerical simulations of the wall y^+ approach accessible in the published work by the same authors [34], a comparison is made between the pressure drop (ΔP) of crude oil obtained from the RSM and that which was calculated theoretically employing the Darcy-Weisbach Eq. (1). The Darcy-Weisbach equation is an empirical equation that relates the loss of pressure caused by friction along the pipe length to the average velocity of the fluid for an incompressible fluid [38]. A comparison is provided below to substantiate the validation of the RSM [38].

$$\frac{\Delta P}{L} = f\frac{\rho u^2}{2D} \tag{1}$$

where L is the length of the pipe (upstream and downstream), D is the internal pipe diameter, ρ is fluid density, u is the mean flow velocity and f is the Darcy friction factor, obtained from Eq. (2) [38].

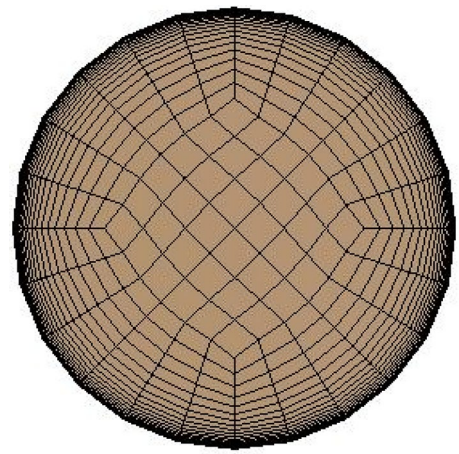

Fig. 2 Fluid Domain Mesh $y^+ \approx 5$ (viscous sublayer)

$$\frac{1}{\sqrt{f}} = -2.0\log10\left(\frac{\varepsilon/D}{3.7} + \frac{2.51}{Re\sqrt{f}}\right) \tag{2}$$

where (ε/D) is the carbon steel relative roughness which equals to 1.18×10^{-4} mm. However, the pressure loss in the 90-degree elbow is obtained by Eq. (3) [39].

$$\Delta P = \frac{1}{2}F_s\rho u^2\frac{\pi R_b}{D}\frac{\theta}{180^0} + \frac{1}{2}k_b\rho u^2 \tag{3}$$

where F_s is the Moody friction factor, ρ the density,u the mean flow velocity,R_b the bend radius, D the pipe diameter, θ the bend angle, and k_b the loss coefficient of bend pipe which equals to 0.3. The k_b is obtained from the loss coefficient of bend pipe graph [39]. The centreline radius of the pipe bend is divided by the internal pipe diameter ($\frac{0.6096}{0.38021} = 1.603$) and k_b is then obtained using the graph.

A comparison between the numerical simulation and theoretical solutions of the pressure loss in the pipe segment with 90-degree elbow for four Reynolds numbers is presented below in Fig. 3. The first Reynolds number (107, 195) is the designed number for the pipeline system of the Mellitah Oil & Gas Company in normal operation. The remaining Reynolds numbers were calculated for the purpose of comparison and to perform additional validations that strengthen the case for using RSM.

The ratio of inertial to viscous forces is known as the Reynolds number. The Reynolds number is a dimensionless quantity used to classify fluid systems where viscosity plays a significant role in regulating fluid velocities or flow patterns and to determine whether a fluid is flowing laminarly or turbulently [38]. The Reynolds number can be obtained by Eq. (4) [38].

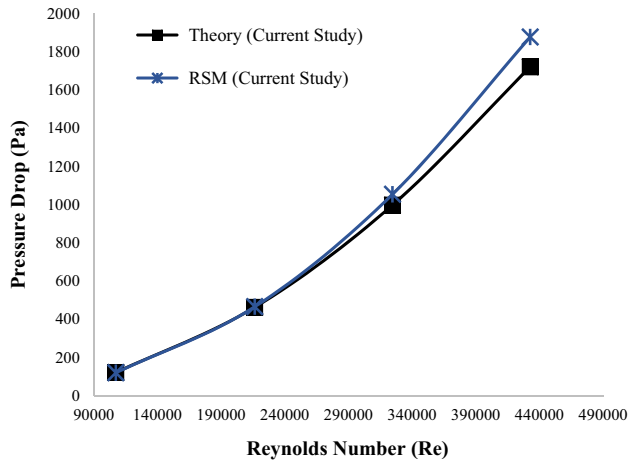

Fig. 3 Comparison between the numerical simulation and theoretical solutions of the pressure loss in the 90-degree pipe elbow segment

$$Re = \frac{\rho v D}{\mu} \tag{4}$$

where ρ is the fluid density, v is the fluid velocity, D is the pipe diameter, and μ is the fluid viscosity.

According to Mellitah Oil and Gas Company operational team, the designed Reynolds number for their pipeline system is in a range of 100,000 and higher numbers are avoided for health and safety reasons and following the standards. In this current study the higher Reynolds number were calculated for the purpose of verification and validation only.

Referring to Fig. 3, for low Reynolds numbers, it shows clear agreement between the RSM and the theoretical results. When the Reynold number is between 1×10^5 and 3×10^5 the RSM performed well with low error percentage. In contrast, discrepancy is observed when the Reynold number is high (between 3.8×10^5 and 5×10^5), though it is still with an acceptable range of error (less than 10%). The RSM, on the other hand, is appropriate for this current study since the Reynolds number is low (1×10^5), and the error percentage in this situation is less than 1%.

For quantitative assessment, more details of the comparison between the numerical simulation and theoretical solutions of the pressure loss are presented in Table 3. This includes the error percentage between the theoretical and simulation results.

The data demonstrated in Table 3 shows good agreement between the RSM and theoretical solutions. The percentage errors were 0.908% and 0.593% for the first and second Reynolds numbers (107,195 and 216,283), respectively. Although the Reynolds numbers increased to 324,425 and 432,566 for the purpose of surveillance, the error percentage is still acceptable and reached 5.669% and 9.078%, respectively. An additional noteworthy observation is that the Darcy friction factor (f) marginally increased with decreasing Reynolds number as illustrated in Table 4. This is because of the inverse relationship between the Reynolds number and friction factor [31].

Table 3 Comparison between the numerical simulation and theoretical solutions of the pressure loss in the pipe segment with 90-degree elbow for four Reynolds numbers

Reynolds number (Re)	Theory	RSM	Error (%)
107,195	121.825	120.719	0.908
216,283	463.322	466.069	0.593
324,425	997.850	1054.421	5.669
432,566	1721.069	1877.313	9.078

Based on the research of the wall y^+ technique accessible in the published work by the same authors [34], as well as the theoretical analysis provided in this section, the RSM that solves the viscous sublayer performed well and provided reliable results. It is employed to investigate the first part of the pipe FSI task, namely, the turbulent pipe flow of crude oil, in normal flow (without leak) condition, in 90-degree elbows. The RSM will be used to predict fluctuations of internal pipe wall pressure caused by changes in flow field parameter (pressure drop) that are induced by leaks. The following sub-section also presents the structure domain, which includes the FSI part, by studying the pipe FIV in normal (without leaks) condition.

2.2 Structure domain

The second part of the problem deals with the structure domain and addresses the vibration response of the external pipe surface produced by the internal pipe wall pressure fluctuations. To computationally investigate the vibration response of the external pipe surface produced by the internal pipe wall pressure fluctuations, certain FEA processes should be followed. This includes the structure meshing, and FEA validation and verification. The procedure typically started with the creation of a CAD model of the system, which was then divided into smaller, finite elements. Each element was then assigned material properties, boundary conditions, and loads. Once the FEA model had all the

Table 4 The relationship between Darcy friction factor (f) and Reynolds Number (Re)

Reynolds number (Re)	Darcy friction factor (f)
107,195	0.0183
216,283	0.0163
324,425	0.0154
432,566	0.0148

required inputs, it would solve the system of equations governing the behaviour of the elements. The results of the analysis would then be post-processed and visualized to identify areas of stress, deformation, or other parameters of interest. Another crucial issue that is carefully considered is the quality of the element shape employed in the FEA mesh. Employing elements with distorted or skewed forms can result in inaccurate FEA findings. Thus, a hexahedral mesh was created with smooth element transitions throughout the structure domain. To provide a more uniform mesh, body and face sizing tools are utilised, particularly in the bend of the pipe. The FEA mesh structure is show in Fig. 4.

Grid Independence Test (GIT) for the structure domain was performed to verify the numerical solution of the FEA after the FSI model was coupled by importing the pressure field from the CFD domain to the structure domain as explained in the previous section. The vibration signal in a form of acceleration (m/s^2) was obtained by the FSI model employing five different meshes based on the total number of elements in each grid taking into consideration the simulation time for each case. The total number of elements varies from grid to another in a range between 8000 and 14,000 elements in each grid. This is demonstrated in Fig. 5.

There was no vast variation in the acceleration values obtained by these five meshes. The percentage difference was calculated and benchmarked against the very fine mesh that contains 13,948 elements. The highest difference was 9% that was obtained from the coarse mesh which comprises 8395 elements. The difference percentage gradually decreased when the total number of elements is increased by employing finer meshes. The FEA solution became more

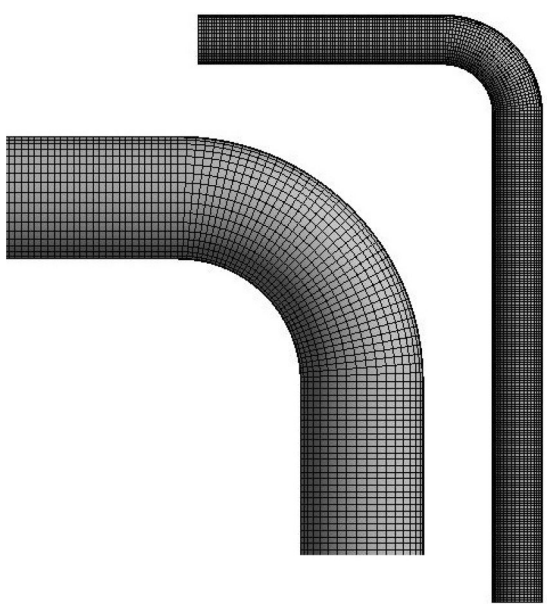

Fig. 4 The FEA mesh structure

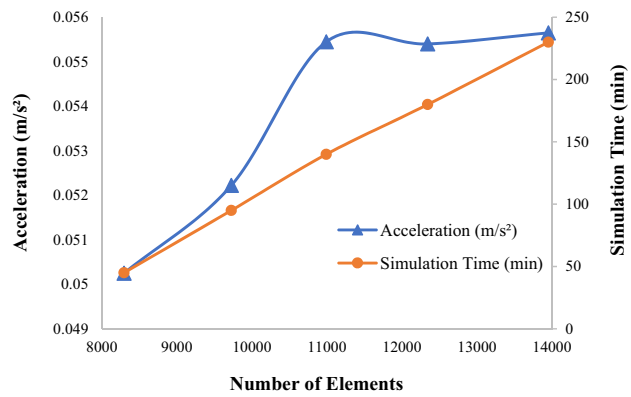

Fig. 5 Grid Independence tests (GIT) for FEA solution

stable when the total number of elements was between 10,989 and 13,948. Therefore, the fine mesh that contains 12,341 elements was selected as optimum with an error of 0.45% from the very fine mesh to balance between the computational cost, time, and mesh quality.

The employed RSM turbulence model and subsequent FSI approaches are initially validated against published experimental and numerical results. The FSI model was validated using experimental and numerical data made available by Pittard et al. [40] prior to beginning the targeted study related to 90-degree pipe elbow flow.

Pittard et al. [40] provided experimental findings that show a substantial link between volume flow rate and a pipe vibration measurement. Pipe vibration is assessed using the standard deviation of the frequency-averaged time-series signal, which is measured using an accelerometer mounted to the pipe. Pittard et al. also demonstrated a numerical FSI model for studying the relationship between pipe wall vibration and the physical properties of turbulent flow. This FSI model uses large eddy simulation (LES) flow models to calculate instantaneous pressure fluctuations in turbulent flow. The numerical LES model findings also show a substantial relationship between pipe vibration and flow rate. According to the results provided by Pittard et al. [40], the pressure variations on the pipe wall have a nearly quadratic relationship with the flow rate. It is concluded that the findings of the experiments and numerical modelling show that the flow rate and the acceleration of pipe vibration have a strong relationship.

Pittard et al. [40] investigated pipe FIV in a small-scale water loop with a pipe length test section of 1.1 m, pipe diameter 0.0762 m and wall thickness of 0.00549 m under different Reynolds numbers. The pipe is simply supported on one side and restrained in the transverse direction from the other side.

After the FSI model of the current research is developed by coupling the RSM that solves the viscous sublayer with

FEA structural model to investigate pipe FIV, it is validated using the experimental and numerical data provided by Pittard et al. [40] as illustrated in Fig. 6.

The RSM that solves the viscous sublayer and is coupled with the FEA structural model performed well when compared against the published data. An excellent agreement between the RSM and the experimental data is observed particularly in low Reynolds numbers. The RSM (current study) performed even better than LES when the Reynold number is low (between 1×10^5 and 3×10^5).

In contrast, the LES performed much better than RSM when the Reynold number is high (between 3.8×10^5 and 5×10^5). This is because LES gives more information on instantaneous fluctuations than RANS and it is better suited for scenarios requiring detailed predictions, such as when the Reynolds number is high, and the turbulence intensity is high [41]. However, this is not the case in the targeted study related to 90-degree pipe elbow flow as the Reynolds number is only 1×10^5. The RSM is suitable for this current study because the Reynolds number is relatively low. Hence the LES is excluded in this current study taking into consideration the high computational cost which may reach ten folds of RSM effort [42].

3 Numerical set up of the VBLD approach

The dynamic response of the pipe segment is simulated using the developed FSI Model of the current research by coupling the RSM that solves the viscous sublayer with FEA structural model. The frequency response data is analysed to detect and classify leaks. The FEA model of the pipe with 90-degree elbow is created, and boundary conditions are set up to simulate the types of loads and constraints that the pipe section is subjected to. A simulated leak is introduced into the model, and a dynamic analysis is run to simulate the vibration response of the pipe to the fluid flow and any leaks. Changes in the frequency response of the pipe elbow can indicate the presence of a leak, and signal processing techniques is used to extract features from the frequency response data to classify the severity of the leak. The validity of the simulation results can be established using experimental data or other analytical methods in future.

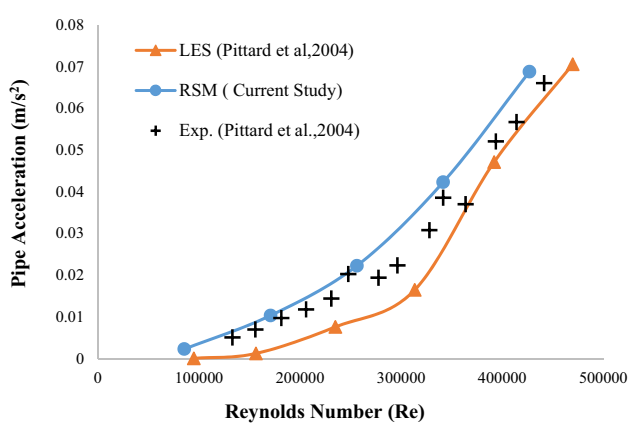

Fig. 6 A comparison of the pipe vibration measurements obtained by the developed FSI model in this current study and the experimental and numerical data by Pittard et al. [41]

Work published in 2020 by Ejeh et al. [33] informed the location of the modelled leak in the current study for a 90 degree pipe elbow. Their findings revealed that the rate of erosion in a pipe is influenced by the particle flow rate, mass, and density. The fluid flowing through the elbow generates a high velocity and pressure gradient, which results in a large centrifugal force acting on the fluid at the bend of the elbow. The centrifugal force causes the fluid to move towards the outer or inner radius of the elbow, which leads to a lower pressure near the centre of the outer or inner radius compared to the surrounding area. The pressure difference across the thickness of the elbow wall can cause stress concentration, which can lead to cracks or other types of damage, resulting in leaks. Therefore, the leak point in this current project is assumed to be in the centre of the elbow, as is shown in Fig. 7 below.

For dependable observation of the computational domain in the abnormal state (with leak) a fine tetrahedral mesh was generated for the leak point and surrounding area to better fit the complexity of the geometry as shown in Fig. 7. Leaks in pipes are modelled based on measurable quantities such as flow rate, pressure, and temperature. In the present study however, the vibration signal of the pipe surface is instead used to detect any leakages.

Six scenarios demonstrated in Table 5 are examined to detect the incidence and severity of a leak based on its size. This is done by using the developed FSI model and performing the same processes as when the pipe FIV is investigated in the normal operation condition (without leak), considering mesh quality.

Figure 8 also illustrates the six different leak cases investigated in the present study starting with no leak (BS case) and moving through increasing leak sizes: LS1—LS5.

The states of the pipe elbow segment are indicated by the scenario ID. The baseline system without leaks is BS, and the leak severity based on its size is LS. The mass flow rate of each leak (leak outlet faces) is obtained by RSM, as illustrated in Table 5. It is noticeable that the mass flow rate in the leak point increases when the leak size grows. This is an additional verification (conservation of mass theory) that supports the use of this FSI model in the current research. The next section presents the results and discussions of this research more in detail.

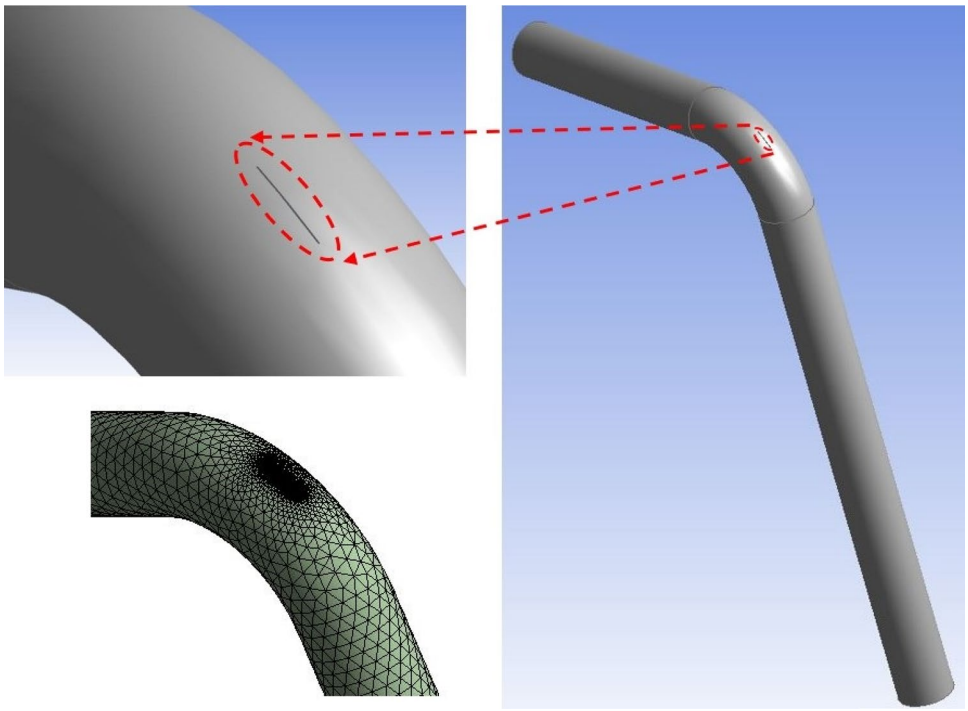

Fig. 7 The leak point in the centre of the elbow

Table 5 All pipe state simulation cases (free leak and leaks occurrence)

Scenario ID	Scenario description	Leak size	Leak mass flow rate (kg/s)
BS	Baseline system without leak	Free leak	0.000
LS1	Leak severity (based on size)	0.002 m × 0.1 m	0.051
LS2	Leak severity (based on size)	0.002 m × 0.2 m	0.148
LS3	Leak severity (based on size)	0.002 m × 0.25 m	0.175
LS4	Leak severity (based on size)	0.002 m × 0.30 m	0.206
LS5	Leak severity (based on size)	0.002 m × 0.35 m	0.245

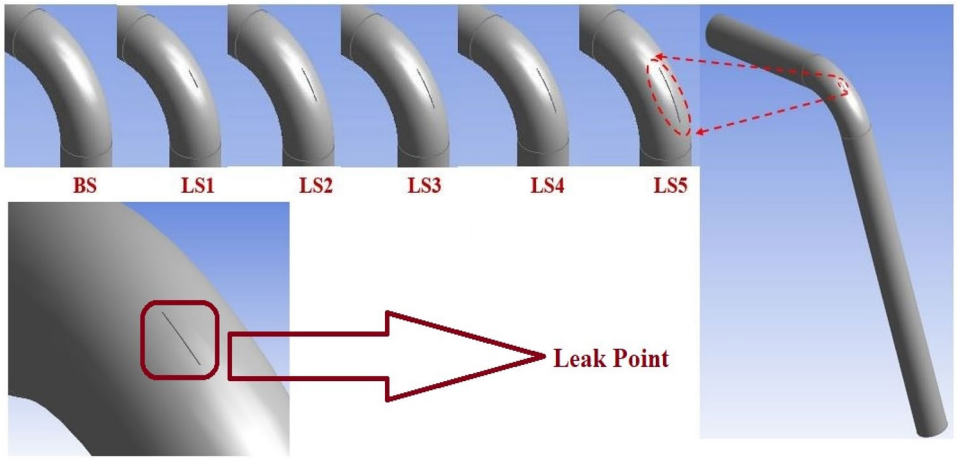

Fig. 8 Leak points and sizes including case IDs

4 Numerical results and discussion

The results of the fluid and structure domains are demonstrated and discussed in this section in normal (without leak) and abnormal (with leaks) conditions. This includes the alteration of flow field behaviour and the pipe vibration response caused by leaks.

4.1 Fluid domain results

The fluid domain is the first part of the problem that is carefully investigated and monitored. The velocity and pressure contours of the pipe segment in normal condition (without leak) are illustrated in Fig. 9a, b, respectively), to demonstrate the fluid flow behaviour in such pipe segments.

In reference to Fig. 9, the foremost feature of flow through a 90- degree pipe elbow is the occurrence of a radial pressure gradient which is formed by centrifugal force acting on the fluid. At the inlet of the elbow bend, the fluid velocity increases near the inner pipe wall (sectional view of elbow) and simultaneously decreases near the outer pipe wall, as highlighted in Fig. 9a, according to the adverse pressure gradient. The highest-pressure concentration occurred in the centre of the elbow at the outer radius (outer pipe wall), as is shown in the pressure contour in Fig. 9b. This resulted in a secondary flow caused by an imbalance between the pressure gradient and centrifugal force. This analysis is based on normal flow condition, in which there were no leaks in the pipe elbow.

The pressure is the main component in the fluid domain and is the force that causes pipe vibration. Observing any alterations in the pressure field caused by leaks is, therefore,

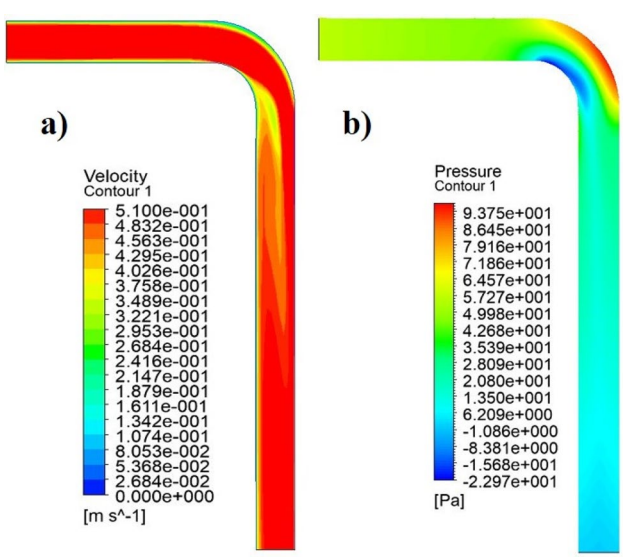

Fig. 9 Velocity and pressure contours of the 90-degree pipe elbow

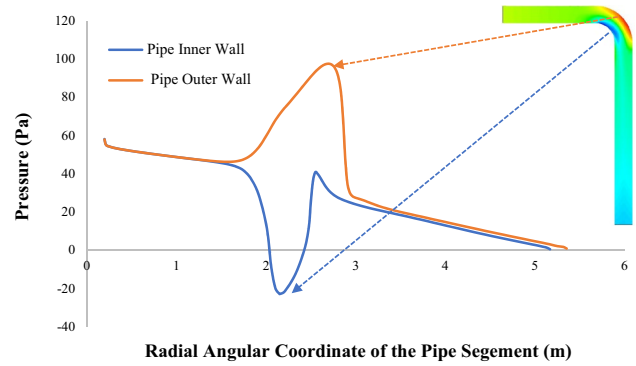

Fig. 10 Pressure distribution along the pipe wall in the case of normal condition (without leak)

essential because pressure distribution is critical for highlighting pipe vibration signal, and it is vital to be plotted in all cases (with and without leaks). The flow field data in the case of abnormal condition (with leaks) is different from the normal condition (without leaks). Figure 10 shows the pressure distribution in the pipe wall (inner and outer section view of the elbow) in normal condition (without leaks). On the other hand, Fig. 11 shows the pressure field during an abnormal condition (with a leak).

In Figs. 10 and 11, the y-axis represents the pressure values distributed through the inner and outer pipe wall. The x-axis represents the radial angular coordinate of the 90-degree pipe elbow segment. It is obvious that the flow is disturbed in the elbow between 1.6 m and 3 m in the x-axis (refer to radial angular coordinate). There was a noticeable pressure drop in the centre of the elbow at the leak point illustrated in Fig. 11, when compared with the normal flow condition (without leak) as is shown in Fig. 10. This sudden alteration in the pressure field caused by the leak has an impact on the pipe vibration signal. The pipe vibration response in the leak scenario is not the same as the case

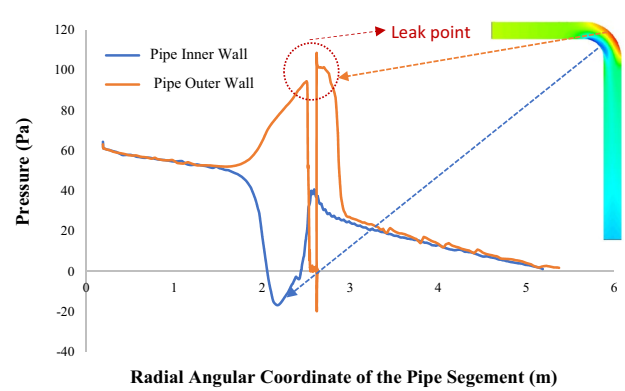

Fig. 11 Pressure distribution along the pipe wall in the case of abnormal condition (with leak)

when there is no leak (normal condition) because the vibration force is the fluid pressure, something which is changed by the leak. This will be demonstrated in the coming section.

For comprehensive observation, the pressure distribution in the outer pipe wall is displayed in all scenarios (with and without leaks), as shown in Fig. 12. This is because the area of the concern is the outer pipe wall (sectional view of elbow) where the leak occurs. The pressure distribution in the inner pipe wall is therefore not represented in this graph.

It is observed that, with the extent of the leakage, the pressure distribution in the centre of the elbow (leak location) changes. The pressure drop area grows in proportion to the size of the leak source. This is demonstrated by the plotted lines in Fig. 12. The displayed continued line (blue line) illustrates the pressure distribution in accordance with normal operation in the baseline scenario (no leak), and no pressure drops owing to leaks are observed.

However, further observation of the fluid domain characteristics is obtained by the velocity profile that have been plotted in all cases (with and without leaks). The location of this velocity profile is chosen to be after the leak location to monitor the effect of leaks occurrence on these examined velocity profiles. The velocity components are plotted in the downstream region (after the elbow) in symmetric lines at X/D = 0 (θ = 90°), as shown in Fig. 13.

The X/D represent the location where the velocity components are plotted, and r/D indicates the inner and outer parts of the centre section of the circular pipe. Again, the change in the velocity profile that is produced by the leak is apparent. The fluid velocity is decreased particularly in the inner pipe wall region. This is because of the small quantities of the mass that flowed out from the leak point which caused a reduction in the fluid velocity in the area around the leak point.

In summary, a comparison between all scenarios (with and without leaks) was carried out in the fluid domain using the pressure and velocity components. The change in the flow behaviour caused by leaks is clear and can be detected. A noticeable pressure drop is detected in the leak point, and this helps in localising the leak. In addition, an alteration in the velocity profile caused by the leaks at the reference location, is also observed. The next subsection will show the results of the structure domain, which is the second part of the problem, and the focus of this research in which it is carefully investigated and monitored.

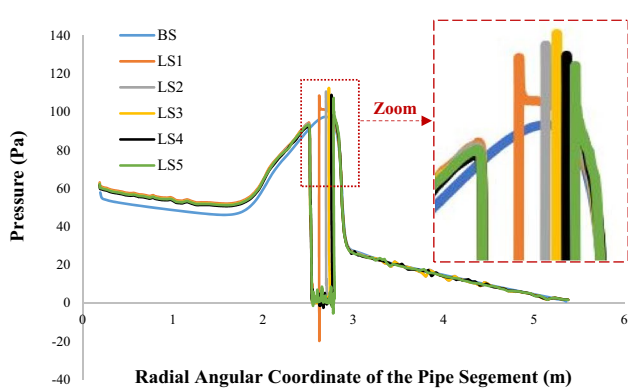

Fig. 12 Pressure distribution in the outer pipe wall in all scenarios (with and without leaks)

4.2 Structure domain results

Since the focus of this research is the VBLD method, the six scenarios illustrated in Table 5 are investigated using the vibration signal analysed in the time and frequency domains. Figure 14 shows the vibration signals in time domain for all cases.

The state of the pipe elbow segments has been previously indicated by the scenario ID. The baseline system without leak is BS while, the LS indicates the leaks and their severity based on size. It is noticeable that the vibration signal changes when a leak occurs. For instance, although the first

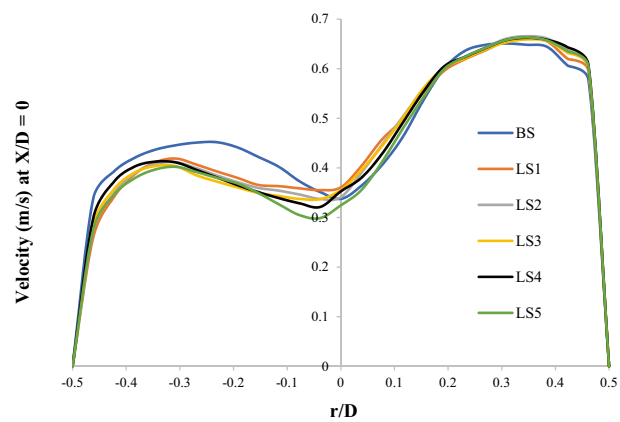

Fig. 13 Comparison of the velocity profile with and without leaks X/D = 0

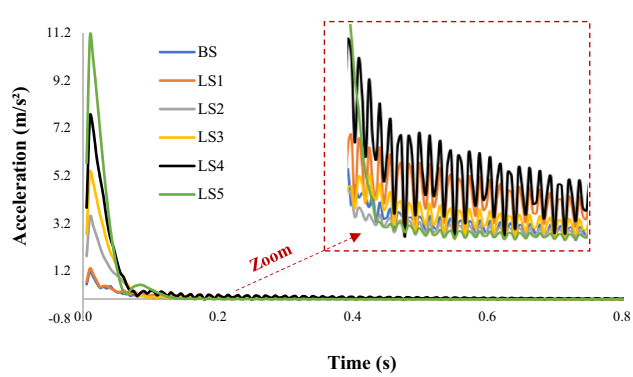

Fig. 14 Vibration signals in the time domain for all cases

leak (LS1) is very small, an alteration in vibration signal is visible when compared to the baseline system (BS) without leaks.

The quantification of vibration signals involves measuring and analysing the characteristics of the signal to understand its frequency, amplitude, and other properties. Since the vibration signal is now measured using numerical simulations, the signal processing techniques are used to remove any noise or interference. The signal is analysed using FFT and time-domain analysis, to determine its frequency and amplitude characteristics. Peak value, and frequency spectrum are calculated to quantify the signal.

Using a frequency-domain graph, you can see how much of the signal, across a variety of frequencies, is present in each specific frequency band. The Fast Fourier Transform (FFT) is a powerful algorithm that computes the Discrete Fourier Transform (DFT) of a set of samples. DFT is a mathematical transformation that divides time domain samples into their frequency components. The time function is transformed using the FFT into a complex valued sum or integral of sine waves with amplitudes and phases that each represent a frequency component. The entire raw vibration data of the pipe segment obtained in the time domain is converted to the frequency domain using FFT for better observation. This is demonstrated in Fig. 15.

With reference to the Fig. 15, all vibration amplitudes (with and without leaks cases) were detected at a frequency of 23 Hz. The vibration amplitudes were measured as total acceleration which are the summation of the three axis (x,y.z). The amplitude of the vibrations changes as the case changes, but the frequency remains constant. This is because the properties of the structure (pipe length, mass, and supports) remained the same, apart from a small leak point where a small amount of fluid mass flowed out, meaning no significant change in the natural frequency of the structure. Despite the small size of the first leak (LS1), a change in the vibration signal can be detected when compared to the normal operating condition (BS). The changes in vibration signal for the remaining cases are clearer due to their combination of larger leak sizes and greater pressure drop magnitudes (vibration force). Again, it is noticeable that the vibration signal rises as the leak size grows. The pipe vibration response is very much dependent on the force (pressure drops due to leaks) that causes the vibration. There is a positive correlation between the vibration signal and these forces. The results of the numerical modelling show that there is a relationship between the pipe vibration and the leak size.

4.3 Leak quantification assessment

Leak Quantification Assessment (LQA) is carried out for the above-mentioned cases by calculating the average of the acceleration serial data obtained in the time domain for each case. This illustrated in Fig. 16.

The vibration amplitude level is expressed in acceleration (m/s^2). Statistical properties of the amplitude are determined by calculating the average of the acceleration serial data obtained in the time domain and are used to describe characteristics of each case signal. The merit of the LQA lies in its sensitivity in detecting leak-induced signals. The results of the study reveal a good correlation between LQA and leak severity, thereby showing that the proposed approach has promise. The LQA has the ability to detect small leaks with greater clarity. Specifically, in a scenario where there is a very small leak (LS1) and no leak present (BS), the difference is not easily distinguishable when the vibration signal is plotted in the time domain (as shown in Fig. 14) or frequency domain (as shown in Fig. 15). However, when the LQA is utilized, the difference becomes much more pronounced.

For additional support of LQA, the difference from the scenario without leak (BS) is calculated as a percentage for each leak severity (LS) as is demonstrated in Table 6.

To conclude, the pipe vibration signal changes when a leak occurs. It is evident that the vibration signal increases as the leak size increases. LQA is more reliable in detecting

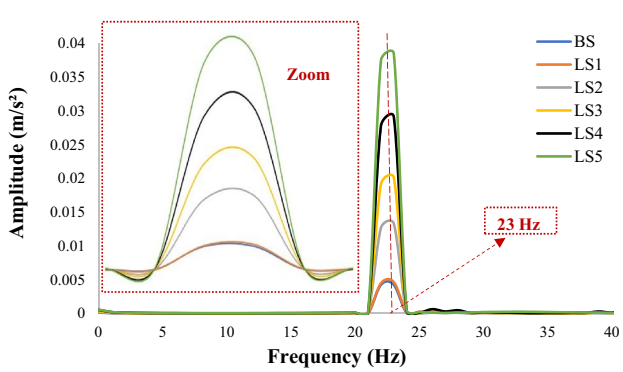

Fig. 15 Vibration signals in the frequency domain for all cases

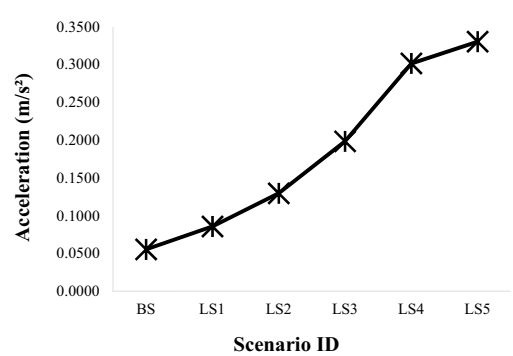

Fig. 16 Leak quantification assessment for all cases

Table 6 All pipe state simulation cases (without leaks and with leaks)

Scenario ID	Acceleration (m/s^2)	Difference from BS Scenario (%)
BS	0.0554	0.00
LS1	0.0857	54.69
LS2	0.1296	133.93
LS3	0.1985	258.30
LS4	0.3015	455.77
LS5	0.3304	496.38

small leaks than using the time and frequency domain data representation. The difference between the scenario without leaks (BS) and the very small leak (LS1) reaches 54.69%, and hence shows the merits of LQA.

5 Conclusions

The present research adds to the growing field of study on vibration-based approaches for detecting leakages in pipelines. Majority of the previous work have focused on experimental investigations in small diameter water pipe networks. This study presents a computational-based VBDL model as a safer, cheaper and less invasive alternative to physical monitoring and testing. CFD simulations are coupled with FEA analysis to carry out vibration monitoring in a 90-degree pipe elbow with the aim of detecting possible leakages. A noticeable pressure drop is observed at modelled leak points and these manifests as changes in vibration signal which can easily be monitored externally using vibration sensors. This offers a cost-effective early detection tool for use in industry and out in the field. The study shows the correlation between pipe vibration and possible leakage points: the vibration signal increases as the leak size increases. The authors recommend carrying out further investigations on a range of pipe elbow angles, spanning from 0 to 180 degrees. This would enable a more comprehensive assessment of the effectiveness of VBLD in detecting leaks in complex pipe system.

Declarations

Conflicts of interest The authors have no conflicts of interest to disclose.

References

1. Meng L, Yuxing L, Wuchang W, Juntao F (2012) Experimental study on leak detection and location for gas pipeline based on acoustic method. J Loss Prev Process Ind 25(1):90–102
2. Mahmutoglu Y, Turk K (2018) A passive acoustic based system to locate leak hole in underwater natural gas pipelines. Digit Signal Process 76:59–65
3. Lim K, Wong L, Chiu WK, Kodikara J (2016) Distributed fiber optic sensors for monitoring pressure and stiffness changes in out-of-round pipes. Struct Control Health Monit 23(2):303–314
4. Png WH, Lin HS, Pua CH, Rahman FA (2018) Pipeline monitoring and leak detection using loop integrated mach zehnder Interferometer optical fiber sensor. Opt Fiber Technol 46:221–225
5. Li H, Xiao D (2009) IIC on and undefined 2009. Morphological filtering assisted field-pipeline small leakage detection. Ieeexplore.ieee.org.
6. Xinhong L, Guoming C, Renren Z, Hongwei Z, Jianmin F (2018) Simulation and assessment of underwater gas release and dispersion from subsea gas pipelines leak. Process Saf Environ Prot 119:46–57
7. Kam SI (2010) Mechanistic modeling of pipeline leak detection at fixed inlet rate. J Pet Sci Eng 70(3–4):145–156
8. Ni S-H, Huang Y-H, Lo K-F, Lin D-C (2010) Buried pipe detection by ground penetrating radar using the discrete wavelet transform. Comput Geotech 37(4):440–448
9. Hoarau Q, Ginolhac G, Atto AM, Nicolas J-M (2017) Robust adaptive detection of buried pipes using GPR. Signal Process 132:293–305
10. Yang Z, Fan S, Xiong T (2010) Simulation and numerical calculation on pipeline leakage process. In 2010 2nd International Symposium on Information Engineering and Electronic Commerce, IEEE, pp 1–5
11. Wan J, Yu Y, Wu Y, Feng R, Yu N (2012) Hierarchical leak detection and localization method in natural gas pipeline monitoring sensor networks. Sensors 12(1):189–214
12. Yin S et al (2018) Mass transfer characteristics of pipeline leak-before-break in a nuclear power station. Appl Therm Eng 142:194–202
13. Turner NC (1991) Hardware and software techniques for pipeline integrity and leak detection monitoring. In Offshore Europe, Society of Petroleum Engineers
14. Murvay P-S, Silea I (2012) A survey on gas leak detection and localization techniques. J Loss Prev Process Ind 25(6):966–973
15. Geiger G, Vogt D, Tetzner R (2006) State-of-the-art in leak detection and localization. Oil Gas Eur Mag 32(4):193
16. Adegboye MA, Fung W-K, Karnik A (2019) Recent advances in pipeline monitoring and oil leakage detection technologies: principles and approaches. Sensors 19(11):2548
17. Salleh HM, Malek NA (2012) Non-revenue water, impact to the service environment and financial
18. Owowo J (2016) Simulation, measurement and detection of leakage and blockage in fluid pipeline systems. University of Manchester
19. Ismail MIM et al (2019) A review of vibration detection methods using accelerometer sensors for water pipeline leakage. IEEE Access 7:51965–51981

20. Choi J, Shin J, Song C, Han S, Il Park D (2017) Leak detection and location of water pipes using vibration sensors and modified ML prefilter. Mdpi.com, doi: https://doi.org/10.3390/s17092104.
21. Gao Y, Muggleton J, Liu Y, Rustighi E (2017) An analytical model of ground surface vibration due to axisymmetric wave motion in buried fluid-filled pipes
22. Keramat A, Tijsseling AS, Hou Q, Ahmadi A (2012) Fluid–structure interaction with pipe-wall viscoelasticity during water hammer. J Fluids Struct 28:434–455. https://doi.org/10.1016/j.jfluidstructs.2011.11.001
23. Zhang T, Tan Y, Zhang X, Zhao J (2015) A novel hybrid technique for leak detection and location in straight pipelines. J Loss Prev Process Ind 35:157–168. https://doi.org/10.1016/j.jlp.2015.04.012
24. Li S, Karney BW, Liu G (2015) FSI research in pipeline systems—a review of the literature. J Fluids Struct 57:277–297. https://doi.org/10.1016/j.jfluidstructs.2015.06.020
25. Ismail MIM, Dziyauddin RA, Samad NAA (2014) Water pipeline monitoring system using vibration sensor. In: ICWiSe 2014–2014 IEEE Conference on Wireless Sensors, pp. 79–84. doi: https://doi.org/10.1109/ICWISE.2014.7042665.
26. Martini A, Troncossi M, Rivola A, Nascetti D (2014) Preliminary investigations on automatic detection of leaks in water distribution networks by means of vibration monitoring. Advances in condition monitoring of machinery in non-stationary operations. Springer, Berlin, pp 535–544
27. Martini A, Troncossi M, Rivola A (2015) Automatic leak detection in buried plastic pipes of water supply networks by means of vibration measurements. Shock Vib 2015:23
28. Yazdekhasti S, Piratla KR, Atamturktur S, Khan AA (2017) Novel vibration-based technique for detecting water pipeline leakage. Struct Infrastruct Eng 13(6):731–742
29. Yazdekhasti S, Piratla KR, Atamturktur S, Khan A (2018) Experimental evaluation of a vibration-based leak detection technique for water pipelines. Struct Infrastruct Eng 14(1):46–55
30. Okosun F, Cahill P, Hazra B, Pakrashi V (2019) Vibration-based leak detection and monitoring of water pipes using output-only piezoelectric sensors. Eur Phys J Spec Top 228(7):1659–1675. https://doi.org/10.1140/epjst/e2019-800150-6
31. Okosun F, Celikin M, Pakrashi V (2020) A numerical model for experimental designs of vibration-based leak detection and monitoring of water pipes using piezoelectric patches. Sensors (Switzerland) 20(23):1–26. https://doi.org/10.3390/s20236708
32. Yang J, Mostaghimi H, Hugo R (2022) Pipeline leak and volume rate detections through artificial intelligence and vibration analysis. Elsevier, Amsterdam
33. Ejeh CJ, Boah EA, Akhabue GP, Onyekperem CC, Anachuna JI, Agyebi I (2020) Computational fluid dynamic analysis for investigating the influence of pipe curvature on erosion rate prediction during crude oil production. Exp Comput Multiph Flow 2(4):255–272. https://doi.org/10.1007/s42757-019-0055-5
34. Abuhatira AA, Salim SM, Vorstius JB (2021) Numerical simulation of turbulent pipe flow with 90-degree elbow using wall y+ approach. ASME 2021 International Mechanical Engineering Congress and Exposition. Nov. 01, 2021. doi: https://doi.org/10.1115/IMECE2021-69986
35. Salim SM, Cheah S (2009) Wall Y strategy for dealing with wall-bounded turbulent flows. In Proceedings of the international multiconference of engineers and computer scientists, Citeseer, 2009, pp. 2165–2170.
36. Ariff M, Salim SM, Cheah SC (2009) Wall y+ approach for dealing with turbulent flow over a surface mounted cube: part 1—low Reynolds number. In Seventh international conference on CFD in the minerals and process industries, pp. 1–6
37. Davidson AA, Salim SM (2018) Wall Y strategy for modelling rotating annular flow using CFD. In: Proceedings of the International MultiConference of Engineers and Computer Scientists
38. Frank WM (2016) Fluid mechanics, 8th edn
39. Jayanti S (2006) Bends (flow and pressure drop in), A-to-Z guide to thermodynamics, heat and mass transfer, and fluids engineering. doi: https://doi.org/10.1615/AtoZ.b.BENFLANDPREDROIN.
40. Pittard MT, Evans RP, Maynes RD, Blotter JD (2004) Experimental and numerical investigation of turbulent flow induced pipe vibration in fully developed flow. Rev Sci Instrum 75(7):2393–2401. https://doi.org/10.1063/1.1763256
41. Versteeg HK, Malalasekera W (2007) An introduction to computational fluid dynamics: the finite volume method. Pearson Education
42. Salim SM (2011) Computational study of wind flow and pollutant dispersion near tree canopies. Division of Environment, University of Nottingham Malaysia Campus, Malaysia. Ph. D thesis